Self-assembling behaviour of Pt nanoparticles onto surface of TiO$_2$ and their resulting photocatalytic activity

M QAMAR and ASHOK K GANGULI[*]

Department of Chemistry, Indian Institute of Technology, New Delhi 110 016, India

Abstract. In the present study, self-assembling behaviour of guest nanoparticles (platinum) onto the surface of host support (titanium dioxide) during photodeposition process as a function of solution pH has been explored in detail by means of transmission electron microscope (TEM). The photocatalytic activity of the resulting bimetallic nanoassembly (Pt/TiO$_2$) was evaluated by studying the degradation of two organic pollutants viz. triclopyr and methyl orange. Microscopic studies revealed that the deposition and/or distribution of Pt nanoparticles onto the surface of TiO$_2$ were strongly guided by the ionization state of support which in turn was regulated by the solution pH of photodeposition process. A direct relationship between the solution pH of deposition process and the photocatalytic activity of resulting bimetallic catalyst has been observed. A mechanism based on the interparticle interaction between TiO$_2$ and hydrolytic products of metal ions has been proposed for the differences in the photocatalytic activity of the resulting nanocomposite.

Keywords. TiO$_2$; sol–gel synthesis; photocatalysis; photodeposition; photocatalytic activity.

1. Introduction

Photocatalysis on semiconductor surfaces, mainly titanium dioxide (TiO$_2$), has attracted considerable attention in recent years as a potential means for the mineralization of organic pollutants present in water and wastewater (Legrini *et al* 1993; Qamar *et al* 2008, 2009; Pan and Zhu 2010) as well as for the direct conversion of solar energy (Fujishima and Honda 1972; Bard 1980; Grätzel 2001; Qamar *et al* 2008; Pan and Zhu 2010). The mechanism constituting heterogeneous photocatalytic oxidation processes has been discussed extensively in the literature (Turchi and Ollis 1990; Matthews and McEvoy 1992; Legrini *et al* 1993; Hoffmann *et al* 1995; Herrmann 1999; Fujishima *et al* 2000; Kamat 2007). One practical problem in using TiO$_2$ is the undesired electron/hole recombination, which in the absence of a proper electron acceptor or donor is extremely efficient and hence, represents the major energy-wasting step, thus limiting the quantum yield. Attempts to employ semiconductor–semiconductor or semiconductor–metal composite nanoparticles have been made to facilitate charge rectification and improve the charge separation efficiency (Tada *et al* 2000; Ivarez-Galván *et al* 2003; Iliev *et al* 2006; Puddu *et al* 2007; Kim and Lee 2009; Kudo and Miseki 2009). The deposition of noble metals onto the surface of semiconductors is beneficial for maximizing the efficiency of photocatalytic reactions (degradation as well as production of hydrogen gas) (Li and

Li 2001; Hufschmidt *et al* 2002; Sano *et al* 2002; Orlov *et al* 2004; Zhang *et al* 2006). The most effective metal to enhance the photocatalytic degradation and hydrogen production, in particular, have been found to be platinum. This metal serves as an electron reservoir and thus promotes an interfacial charge-transfer process leading to higher efficiency.

Recently, few articles have appeared in the literature describing different aspects of Pt/TiO$_2$ nanocomposite, such as the inter-relationship between oxidation states of deposited Pt and photocatalytic activity of Pt/TiO$_2$ substrate specificity (Teoh *et al* 2007), the effect of Pt oxidation states on TiO$_2$ (Lee and Choi 2005), inter-relationship between Pt and type of TiO$_2$ (Hufschmidt *et al* 2002). In most of the studies, synthesis of Pt/TiO$_2$ assembly has been carried out following photodeposition method, a versatile route to synthesize the bimetallic nanoassembly involving noble metals and metal oxides. During photodeposition of metals onto the surface of semiconductors, an important parameter in the photocatalytic reactions taking place on the particulate surfaces is the pH of the solution, since it dictates surface properties of the catalyst which in turn may affect the interparticle interaction. In spite of the appearance of a number of articles in the literature based on the surface modification of TiO$_2$ with Pt, the self-assembling behaviour of Pt metal onto the surface of TiO$_2$ with respect to solution pH and their corresponding photocatalytic activity remains unexplored.

In the present study, therefore, an attempt was made to furnish a direct relationship between solution pH and self-assembling behaviour of Pt onto the surface of TiO$_2$ as well as photocatalytic activity of resulting bimetallic nanoassembly. The effect of platinum loadings such as 0·5, 1·0, 1·5,

[*]Author for correspondence (ashok@chemistry.iitd.ac.in)

2·0 and 2·5 wt% on the photocatalytic activity of TiO$_2$ was studied.

2. Experimental

2.1 *Synthesis of catalysts*

The synthesis of TiO$_2$ samples was carried out using the sol–gel technique. In a typical synthesis, TiO$_2$ was obtained by hydrolyzing titanium isopropoxide (Aldrich, 97%) with an equal volume ratio of water and isopropanol. The white precipitate was centrifuged and dried at 110 °C overnight and then calcined at various temperatures.

2.2 *Photodeposition of metals*

Photodeposition of metals onto the surface of titanium dioxide was performed using a modified process described elsewhere (Siemon *et al* 2002). A typical photodeposition was carried out using an immersion well photochemical reactor made of Pyrex glass equipped with a magnetic stirring bar, a water circulating jacket and an opening for the supply of gases. A detailed description of the photochemical reactor was presented in our earlier paper (Qamar and Muneer 2005). For irradiation experiments, 240 ml of water was taken into the photoreactor and the required amount of K$_2$PtCl$_6$ (wt%), photocatalyst (500 mg), and ethanol as an electron donor (at a molar ratio ethanol:metals salts = 500:1) was added and the solution was stirred and purged throughout the reactions with high purity nitrogen gas to remove the oxygen. Irradiation was carried out using 125 W medium pressure mercury lamp (Philips) for 6 h. pH of the reaction mixture was adjusted to the desired value by adding a dilute aqueous solution of HNO$_3$ or NaOH. After irradiation, the metal loaded catalyst was washed and separated through centrifugation and dried at 110 °C overnight.

2.3 *Characterization methods*

The characterization of these samples was carried out by employing powder X-ray diffraction (PXRD, with Ni-filtered CuKα radiation, Bruker D8 Advance), transmission electron microscopy (TEM, FEI Technai G^2 20 operated at 200 kV), energy dispersive X-ray spectroscopy (EDX) and UV–Visible spectrophotometer.

2.4 *Evaluation of photocatalytic activity*

The photocatalytic activity was evaluated using the same photochemical reactor as described above. For irradiation experiments, a 250 ml solution of desired concentration of triclopyr and methyl orange (0·15 mM of each) was taken into the vessel and required amount of the catalyst (1 g L^{-1}) was added into the solution. Before irradiation, the solution was magnetically stirred for 30 min to allow equilibration
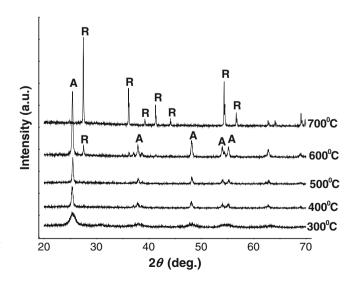
of the system. Irradiation was carried out using a 125 W medium pressure mercury lamp (Philips) for 2 h and samples (5 ml) were drawn from the photoreactor before and at regular intervals during irradiation.

The degradation rate for the decomposition (decrease in absorption intensity vs irradiation time) of the pollutants was monitored by measuring the change in absorbance on a UV–Vis spectrophotometer. The absorbance of triclopyr and methyl orange was followed at 233·5 and 464 nm (λ max) wavelengths, respectively after proper dilution with water. The initial absorbance, without any irradiation, of both the pollutants was found to be more than 2. Hence, a proper dilution was carried out with water so that the initial absorbance becomes ∼1·9 and Beer–Lamberts law could be followed. The dilution factor was kept constant for all non-irradiated as well as irradiated samples. For each experiment, the rate constant was calculated from the initial slope obtained by linear regression from a plot of the natural logarithm of the absorbance of the pollutants as a function of irradiation time. The degradation rates were calculated in terms of M min^{-1}.

3. Results and discussion

3.1 *Effect of calcination temperature on photocatalytic activity*

The change in crystal structure of TiO$_2$ as a function of calcination temperature was followed by XRD and has been shown in figure 1. The photocatalytic decomposition of triclopyr in the presence of different calcined TiO$_2$ samples was investigated and the values obtained are listed in table 1. The photocatalytic activity was found to increase with increase in calcination temperature presumably due to the formation of anatase phase and improvement of its crystallinity. The highest activity was observed at 400 °C followed by a decrease at higher temperatures and the samples calcined at 400 °C

Figure 1. XRD patterns of TiO$_2$ samples obtained after calcination at different temperatures: (A) anatase and (R) rutile.

Table 1. Photocatalytic degradation of triclopyr in presence of various calcined samples of TiO_2.

Calcination temperature (°C)	Degradation rate (M min^{-1} × 10^{-3})
300	0·0098
400	0·0183
500	0·0137
600	0·0106
700	0·0054
800	0·0013

Table 2. Photocatalytic degradation of triclopyr in presence of TiO_2 calcined at 400 °C containing varying amounts of platinum.

Catalyst	Degradation rate (M min^{-1} × 10^{-3})
TiO_2	0·0183
0·5 wt% Pt/TiO_2	0·0327
1·0 wt% Pt/TiO_2	0·0526
1·5 wt% Pt/TiO_2	0·0436
2·0 wt% Pt/TiO_2	0·0360
2·5 wt% Pt/TiO_2	0·0259

showed best photocatalytic activity followed by a decrease at higher temperatures. This phenomenon could be explained in terms of crystallinity, surface area and particle size of samples which in turn regulate the photocatalytic efficiency of the sample. As the calcination temperature is increased, surface area and particle size decreases while crystallinity of materials improves. The high photocatalytic activity shown by sample calcined at 400 °C seems to be due a compromise between the surface area and degree of crystallinity. On the other hand, low activity shown by the sample calcined at 300 °C compared to 400 °C calcined sample could be due to its poor degree of crystallinity, which was not compensated by the positive effect given by its high surface area. The decrease in photocatalytic activity of the samples at higher temperatures such as 600 and 700 °C could be due to the formation of less photocatalytically active rutile phase of TiO_2 as evident from figure 1 (Sclafani and Hermann 1996; Qamar *et al* 2008).

3.2 *Effect of metallization*

Since the highest photocatalytic activity was shown by TiO_2 calcined at 400 °C, varying amounts of platinum (0·5, 1·0, 1·5, 2·0 and 2·5 wt%) were photodeposited onto the surface of this sample. The estimated range of deposited platinum nanoparticles was found to be 2–4 nm. Presence of platinum nanoparticles onto the surface of the support was also confirmed by EDX (figure 5). Pt nanoparticles remain present onto the surface of metal oxides either in metallic form (Pt^0) or PtO or PtO$_2$ depending on the experimental conditions. There is no chemical bonding between Pt and TiO_2 surface but Pt remains adhered onto the oxide surface by a well known interaction called strong metal (Pt)-support (TiO_2) interaction (SMSI) (Spencer 1985; Lewera *et al* 2011). The photocatalytic degradation rates of triclopyr in the presence of Pt-modified samples are presented in table 2. The maximum degradation of triclopyr was obtained with 1 wt% metal loading followed by a decrease at higher metal amount. The enhancement in decomposition rate of organic pollutants in the presence of metallized TiO_2 has been discussed previously by several authors (Legrini *et al* 1993; Sun *et al* 2003; Ishibai *et al* 2007; Lam *et al* 2007; Teoh *et al* 2007; Yu and Chuang 2008; Pan and Zhu 2010). The enhancement in decomposition rate

of organic pollutant in the presence of metallized metal oxides may be mainly attributed to the formation of a Schottky barrier between the metal and the semiconductor (Hufschmidt *et al* 2002). When the platinum particles are deposited onto the surface of TiO_2, a Schottky barrier formed at the interface of TiO_2 and Pt metal particles, resulting in an efficient channeling of excited conduction band electrons from the bulk of TiO_2 to the newly formed interface. As a result, the electron density in TiO_2 particles decreases which in turn prevents the electron–hole pair recombination. As a result, higher photocatalytic activity was observed. The decrease in degradation rate at higher metal amounts may be rationalized in terms of screening or shadowing of catalyst surface. A higher content of metal can prevent the incident photons from reaching the surface of the catalyst thereby decreasing the photocatalytic performance.
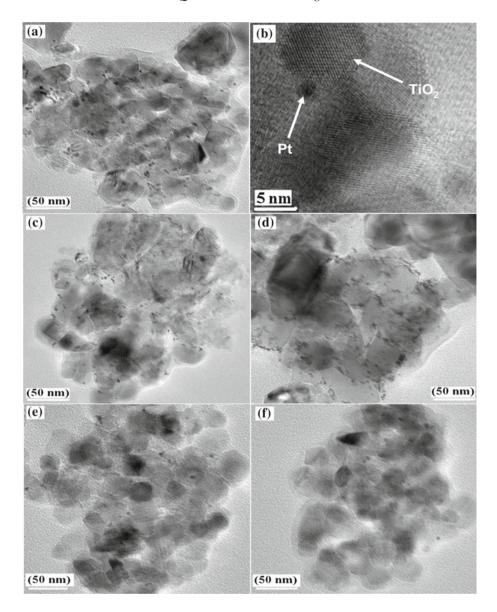
3.3 *Effect of solution pH during photodeposition process*

Pt/TiO_2 samples prepared at different pH values were analysed using TEM and the resulting images are illustrated in figure 2. The histograms of platinum particle size distribution as a function of solution pH are shown in figure 3. Small black dots were platinum particles. In an acidic medium (pH ≤ 5), platinum nanoparticles were distributed homogeneously. When the pH was increased (nearly neutral pH), most of the platinum particles tend to agglomerate and align themselves on the boundary of TiO_2 particles (figure 2(d)). In alkaline conditions (pH ≥ 9), shape of platinum nanoparticles was spherical and agglomeration of platinum was not observed, but the number of platinum particles was much less than those obtained at other pH values.

This phenomenon may be rationalized in terms of surface properties of TiO_2 and hydrolytic behaviour of $PtCl_6^{2-}$ in aqueous solution. In case of TiO_2, zero point of charge (pH$_{zpc}$) is at a pH of 6·25. Hence, at more acidic pH values, the particle surface is positively charged, while at pH values above 6·25, it is negatively charged (Muneer *et al* 2005). The ionization state of the surface of the photocatalyst may be understood by (1) and (2):

$$TiOH + H^+ \longrightarrow TiOH_2^+, \tag{1}$$

$$TiOH + OH^- \longrightarrow TiO^- + H_2O. \tag{2}$$

Figure 2. TEM micrographs of TiO$_2$ calcined at 400 °C containing 1 wt% Pt prepared at various solutions of pH; (**a**) pH $\sim$ 3·1, (**b**) HRTEM of sample (**a**), (**c**) pH $\sim$ 5·4, (**d**) pH $\sim$ 7·2, (**e**) pH $\sim$ 9·3 and (**f**) pH $\sim$ 11·6.

In an aqueous solution, PtCl$_6^{2-}$ undergoes a sequential hydrolysis to give various hydrolytic products as mentioned below in (3)–(8) (Cox *et al* 1972; Jin *et al* 1994):

$$PtCl_6^{2-} + OH^- = Pt(OH)Cl_5^{2-} + Cl^-, \qquad (3)$$

$$Pt(OH)Cl_5^{2-} + OH^- = Pt(OH)_2Cl_4^{2-} + Cl^-, \qquad (4)$$

$$Pt(OH)_2Cl_4^{2-} + OH^- = Pt(OH)_3Cl_3^{2-} + Cl^-, \qquad (5)$$

$$Pt(OH)_3Cl_3^{2-} + OH^- = Pt(OH)_4Cl_2^{2-} + Cl^-, \qquad (6)$$

$$Pt(OH)_4Cl_2^{2-} + OH^- = Pt(OH)_5Cl^{2-} + Cl^-, \qquad (7)$$

$$Pt(OH)_5Cl^{2-} + OH^- = Pt(OH)_6^{2-} + Cl^-. \qquad (8)$$

Based on the above chemical equations, it may be understood that in an acidic condition, the positively charged TiO$_2$ surface will facilitate adsorption of PtCl$_6^{2-}$ and its hydrolyzed ions (the concentration of anions will be higher on the surface), thereby increasing the entrapment of excited conduction band electrons resulting in a high deposition rate of platinum nanoparticles on the support. When the value of solution pH is closer to the isoelectric point of TiO$_2$ (6·25), TiO$_2$ particles tend to aggregate and only a limited surface is available for platinum nanoparticles to be deposited. As a result, most of the platinum particles were present on the surface of support in the form of agglomerates. In a basic condition, on the other hand, the negatively charged surface of TiO$_2$ will explain the anchoring behaviour of platinum nanoparticles. On a negatively charged surface of TiO$_2$, the concentration of PtCl$_6^{2-}$ and its hydrolyzed products is
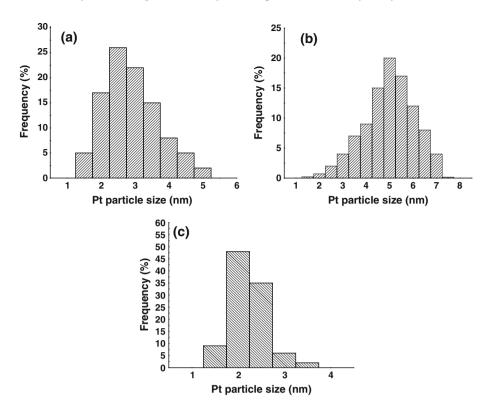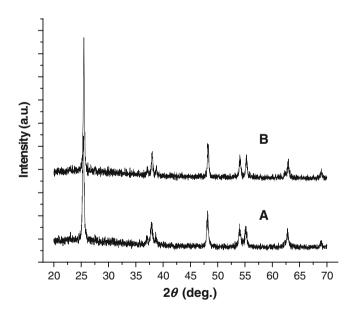
Figure 3. (**a**)–(**c**) Histogram of platinum particle size distribution as a function of solution pH.

Figure 4. XRD patterns of (**A**) TiO$_2$ sample calcined at 400 °C for 2 h and (**B**) TiO$_2$ sample (calcined at 400 °C for 2 h) after modification with 1 wt% Pt.

expected to be low, which in turn led to the low deposition rate that resulted in a smaller number of platinum particles.

XRD patterns of TiO$_2$ before and after Pt deposition (1 wt%, under acidic environment) is given in figure 4. No obvious difference was observed between the two spectra. When the impurity level onto the surface of any sample, Pt in

this case, remains less than 5%, it is less likely to be detected by XRD but the presence of Pt onto the surface of TiO$_2$ was confirmed by TEM and EDX, as presented in figures 2 and 5, respectively.

The photocatalytic activity of various platinized TiO$_2$ samples prepared at different pH values during photodeposition process was tested not only for the degradation of triclopyr but also for a dye viz. methyl orange and obtained results are presented in figures 6 and 7, respectively. In both the cases (triclopyr and methyl orange), activity of the resulting Pt/titania nanocomposites has been found to be very much dependant on the synthesis condition (solution pH during photodeposition process) or in other words, on the distribution of platinum nanoparticles onto the surface of TiO$_2$. The catalyst prepared in an acidic environment (pH of 3·1) showed highest activity as compared to those prepared under basic environment. This behaviour may be attributed to the number, size, size distribution, shape and morphology of platinum particles deposited onto the surface of the TiO$_2$ support. It can be seen from figures 2(a) and 5(a) that the number of deposited platinum particles was higher, their size was small and their shape and morphology was uniform, which in turn led to higher efficiency of the catalyst. In contrast, as the pH was increased, most of the platinum particles were present in the form of agglomerates (as directed by surface of the support), thereby limiting the efficiency of the nanocomposite. In addition, though the particles were uniform and small, the possible reason for high retardation of degradation rate (even less than the bare TiO$_2$) in the presence of samples prepared under higher alkaline medium (pH 9·3 and

11·6) may be due to the formation of platinum oxides such as PtO and PtO$_2$. Previously, it has been found that PtO and PtO$_2$ were the main deposited species in a more basic environment involving the reaction of hydrolyzed platinum complexes with valence band holes as indicated in the following (Jin *et al* 1994; Zhang *et al* 2004):

$$Pt(OH)_4Cl_2^{2-} + 4hvb^+ \longrightarrow PtO_2 + 4H^+ + O_2 + 2Cl^-.$$

Pt^0/TiO$_2$ has been found to be more photocatalytically active than Pt^{II}/TiO$_2$ and Pt^{IV}/TiO$_2$ for the degradation of various chlorinated contaminants (Kim and Choi 2002). Pt^{II}/TiO$_2$ and Pt^{IV}/TiO$_2$ can undergo consecutive reduction/oxidation cycles involving an appreciable amount of excited charge carriers thereby facilitating the process of electron–hole pair recombination which in turn results in a lower efficiency of the assembly.
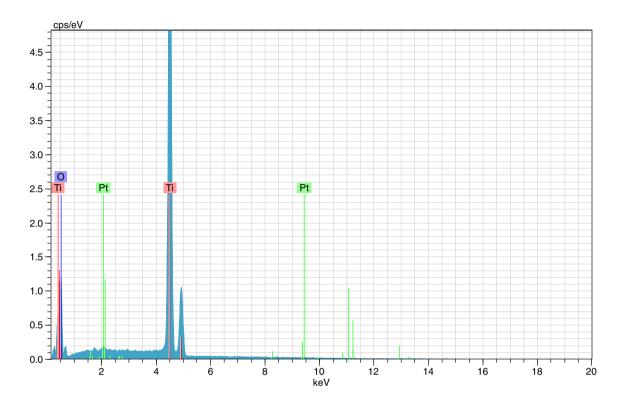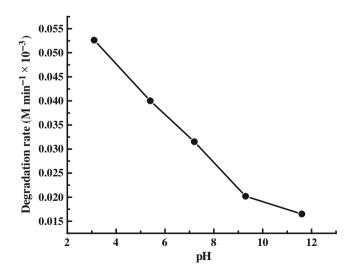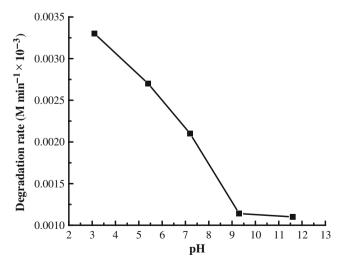

Figure 5. EDX spectra of TiO$_2$ sample after modification with 1 wt% Pt.

Figure 6. Variation in photocatalytic activity of Pt/TiO$_2$ nanocomposite prepared at different pH for decomposition of triclopyr.

Figure 7. Variation in photocatalytic activity of Pt/TiO$_2$ nanocomposite prepared at different pH for decomposition of methyl orange.

4. Conclusions

The present study furnished a direct relationship between the self-assembling behaviour of Pt nanoparticles on the surface of TiO$_2$ and value of solution pH during photodeposition process. An acidic environment (pH $\sim$ 3) favoured the anchoring and fine distribution of platinum nanoparticles onto the surface of TiO$_2$ owing to better interparticle interaction between TiO$_2$ and hydrolytic products of metal ions. A linear relationship was obtained between the solution pH of the deposition process and photocatalytic activity of the corresponding bimetallic nanoassembly (Pt/TiO$_2$), i.e. the photocatalytic activity decreased with the increase in pH. Since the morphology and concentration of coated metals are important from application point of view, the present observations could be modified and utilized to control the concentration of host metals on the surface of support to achieve different kinds of solid-supported metal nanoassembly in single step.

Acknowledgments

References

Bard A J 1980 *Science* **207** 4427

Cox L, Peter D C and Wehry E L 1972 *J. Inorg. Nucl. Chem.* **86** 297

Fujishima A and Honda K 1972 *Nature* **238** 37

Fujishima A, Rao T N and Tryk D A 2000 *J. Photochem. Photobiol. C: Photochem. Rev.* **1** 1

Grätzel M 2001 *Nature* **414** 338

Herrmann J M 1999 *Catal. Today* **53** 115

Hoffmann M R, Martin S T, Choi W and Bahnemann D W 1995 *Chem. Rev.* **95** 69

Hufschmidt D, Bahnemann D, Testa J J, Emilio C A and Litter M I 2002 *J. Photochem. Photobiol. A: Chem.* **148** 223

Iliev V, Tomova D, Bilyarska L, Eliyas A and Petrov L 2006 *Appl. Catal.* **B63** 266

Ishibai Y, Sato J, Akita S and Miyagishi T N S 2007 *J. Photochem. Photobiol. A: Chem.* **188** 106

Ivarez-Galván M C A, de la Pena O'Shen V A, Fierro J L G and Arias P L 2003 *Catal. Commun.* **4** 223

Jin Z, Chen Z, Li Q, Xi C and Zheng X 1994 *J. Photochem. Photobiol. A: Chem.* **81** 177

Kamat P V 2007 *J. Phys. Chem.* **C111** 2834

Kim S and Choi W 2002 *J. Phys. Chem.* **B106** 13311

Kim S and Lee S-K 2009 *J. Photochem. Photobiol.* **A23** 145

Kudo A and Miseki Y 2009 *Chem. Soc. Rev.* **38** 253

Lam S W, Chiang K, Lim T M, Amal R and Low G K-C 2007 *Appl. Catal.* **B72** 363

Lee J and Choi W 2005 *J. Phys. Chem.* **B109** 7399

Legrini O, Oliveros E and Braun A M 1993 *Chem. Rev.* **93** 671

Lewera A, Timperman L, Roguska A and Alonso-Vante N 2011 *J. Phys. Chem.* **C115** 20153

Li X Z and Li F B 2001 *Environ. Sci. Technol.* **35** 2381

Matthews R W and McEvoy S R 1992 *J. Photochem. Photobiol. A: Chem.* **64** 231

Muneer M, Qamar M, Saquib M and Bahnemann D 2005 *Chemosphere* **61** 457

Orlov A, Jefferson D A, Macleod N and Lambert R M 2004 *Catal. Lett.* **92** 41

Pan C and Zhu Y 2010 *Environ. Sci. Technol.* **44** 5570

Puddu V, Mokaya R and Li Puma G 2007 *Chem. Commun.* **45** 4749

Qamar M *et al* 2008 *Catal. Today* **131** 3

Qamar M and Muneer M 2005 *J. Hazard. Mater.* **120** 219

Qamar M, Gondal M A and Yamani Z H 2009 *Catal. Commun.* **10** 1980

Sano T, Kutsunga S, Negishi N and Takeuchi K 2002 *J. Mol. Catal.* **A189** 263

Sclafani A and Hermann J M 1996 *J. Phys. Chem.* **100** 13655

Siemon U, Bahnemann D, Testa J J, Rodriguez D, Litter M I and Bruno N 2002 *J. Photochem. Photobiol. A: Chem.* **148** 247

Spencer M S 1985 *J. Catal.* **93** 216

Sun B, Vorontsov A V and Smirniotis P G 2003 *Langmuir* **19** 3151

Tada H, Teranishi T K, Yo-ichi I and Ito S 2000 *Langmuir* **16** 3304

Teoh W Y, Madler L and Amal R 2007 *J. Catal.* **251** 271

Turchi C S and Ollis D F 1990 *J. Catal.* **122** 178

Yu Z and Chuang S S C 2008 *Appl. Catal.* **B83** 277

Zhang C, He H and Tanaka K 2006 *Appl. Catal.* **B65** 37

Zhang F, Chen J, Zhang X, Gao W, Jin R, Guan N and Li Y 2004 *Langmuir* **20** 9329